Mechanical properties of cellulose aerogels and cryogels

Nela Buchtová, Christophe Pradille, Jean-Luc Bouvard, Tatiana Budtova

Mechanical properties of cellulose aerogels and cryogels

Nela Buchtová[1], Christophe Pradille[2], Jean-Luc Bouvard[1], Tatiana Budtova[1]*

1 - MINES ParisTech, CEMEF - Centre de Mise en Forme des Matériaux, CNRS UMR 7635, PSL Research University, CS 10207 rue Claude Daunesse, 06904 Sophia Antipolis, France

2 - Mat Xper, 19 Traverse du Barri, 06560, Sophia Antipolis, France

Corresponding author: Tatiana Budtova

E-mail: tatiana.budtova@mines-paristech.fr

Abstract

Highly porous and lightweight cellulose materials were prepared via dissolution–coagulation and different drying routes. Cellulose of three different molecular weights was dissolved in ionic liquid/dimethyl sulfoxide mixture. Drying was performed either with supercritical CO_2 resulting in “aerogels”, or via freeze-drying resulting in “cryogels”. The influence of cellulose molecular weight, concentration and drying method on the morphology, density, porosity and specific surface area was determined. The mechanical properties of cellulose cryogels and aerogels under uniaxial compression were studied in details and analyzed in the view of existing models developed for porous materials. It was demonstrated that the Poisson’s ratio of cellulose aerogels is not equal to zero, contrary to what is usually reported in literature, but decreases with density increase. Compressive modulus and yield stress of cryogels turned out to be higher than those of aerogels taken at the same density. This was interpreted by different morphology of the porous materials studied.

Keywords: Cellulose, aerogels, cryogels, porosity, morphology, mechanical properties

1. Introduction

Lightweight cellulose materials, aerogels and foams, have been attracting a lot of attention as they can be used for absorption and adsorption, as carriers of drugs, as scaffolds and as carbons for electrochemical applications when pyrolysed.[1-3] These highly porous materials can be obtained either from “nanocellulose” (various forms of nanofibrillated cellulose (NFC) and nanocrystals) or via cellulose dissolution-coagulation route. In all cases, the precursor of the dry foam or aerogel is “wet” cellulose, often with water within the pores, and thus called “hydrogel”. Compared to its “wet” counterpart, dry porous cellulose has several advantages: i) shape and morphology stability in time; ii) long storage time without the need of protection against solvent evaporation and growth of bacteria; iii) low to very low density which ensures easy transportation and iv) possibility of making various nanostructured hybrid and composite organic-organic and organic-inorganic materials.

Drying of the “wet” cellulose precursor is a critical step which determines material’s final morphology and properties. There are two main drying ways which allow keeping high porosity: freeze-drying (or lyophilisation) and drying in supercritical conditions (usually with CO_2). In the following, for simplicity, we will call the freeze-dried material “cryogel” and the supercritically dried material “aerogel”. In most of the cases, if a cellulose hydrogel is freeze-dried, the morphology of the cryogel is a replica of sublimated ice crystals with pore size from few microns to several hundreds of microns, very low density and a rather low specific surface area (around few tens of m^2/g). This low specific surface area is due to the loss of nanostructure in pore walls as cellulose fibrils are compressed by growing ice crystals. To suppress the growth of the ice crystals, freeze-drying is performed from tert-butanol[4] or using spray-freeze-drying,[5] both preserving the nanostructure of the cellulose cryogel’s precursor and leading to separated nanofibrils and thus higher specific surface area. When performing drying with supercritical CO_2 ($scCO_2$), cellulose aerogels are lightweight, nanostructured and with very high specific surface areas of several hundreds of m^2/g.[1-3]

In any practical application, the understanding and control of material’s mechanical properties is a prerequisite. For porous structures, the utmost importance is the correlation of

mechanical properties with material's morphology and density. For classical silica aerogels, a lot of experimental work and modelling were performed leading to a good understanding of structure-properties relationship, including the influence of various parameters of silica sol-gel process, formation of clusters, aerogels' morphology (porosity, connectivity, fractal dimension, pore size, structure of pore walls, etc.) and correlation with materials' mechanical properties.[6,7] However, for cellulose aerogels and cryogels (or foams), there is still a long way to do in the understanding of materials' mechanical properties and their correlation with morphology. One of the reasons is a huge variety of processing parameters leading to very different morphologies and properties: type of cellulose (cellulose I or cellulose II) and its concentration, cellulose solvent and non-solvent, pathways in structure formation of the precursor (gelation or non-solvent induced phase separation), drying route, crystallinity of the final material, etc. Another problem with highly porous polysaccharide materials is the difficulty in characterization of their pore size distribution with standard methods.[3] For instance, the BJH method based on nitrogen adsorption-desorption distinguishes only 10-20% of the total pore volume as it takes into account only mesopores and small macropores while most of bio-aerogels possess many large macropores.[5,8-10] Mercury porosimetry leads to sample compression instead of mercury penetration within the pores.[9]

Till now, the majority of the mechanical properties of cellulose cryo- and aerogels have been obtained from uniaxial compression tests. Moreover, various sample geometries have been used which may influence the results and their interpretation. Most of the works suppose zero Poisson's ratio without a detailed analysis of the evolution of sample's dimensions. All authors agree that compressive modulus increases with the increase of material's density, as expected. Many suggest a power law dependence of modulus and strength on the density,[11-14] as in the case of classical foams and aerogels.[6,15-20] However, a huge variety of exponents, from linear to power 4, were reported even for materials within the same family (for example, for cellulose II-based aerogels). Recently, modelling of a stress-strain compression curve of cellulose II aerogels (made via the dissolution in $Ca(SCN)_2 \cdot 6H_2O$ and in $ZnCl_2 \cdot 4H_2O$ and dried with $scCO_2$) has been suggested.[21] Those aerogels had a net-

like morphology, and the model based on the non-linear bending and collapse of cells of different sizes gave a good match with the experimental stress-strain behavior. The experimental compressive modulus was approximated by a linear dependence on aerogel's density. Using the same solvent ($ZnCl_2 \cdot 4H_2O$), another work demonstrated that the modulus of cellulose aerogels strongly increases as a function of density with exponents varying from 2.6 to 4.6 depending on the type of non-solvent used.[22] The modulus of cellulose II-based aerogels made via the dissolution either in NaOH-water or in ionic liquid was also shown to be power-law dependent on aerogel's density with exponent varying from 2 to 3.[13] When cellulose aerogels were made using an emulsion templating method, the compressive modulus was shown to depend on material's morphology with thicker pore walls resulting in higher modulus value.[23]

The goal of the present work was to perform a systematic analysis of the mechanical properties of two types of cellulose porous materials, aerogels and cryogels, and to correlate their mechanical properties to materials' morphology and density. We used the same approach in the preparation of the aerogels' and cryogels' precursors as described in ref. 24 where microcrystalline cellulose was dissolved in a model solvent, a mixture of 1-ethyl-3-methylimidazolium acetate ionic liquid ([Emim][OAc]) and dimethyl sulfoxide (DMSO), and then coagulated in ethanol. In the present work, cellulose of three different molecular weights at various concentrations was used in order to study also the influence of the cellulose chain length. Starting from the same "wet" precursor, drying with $scCO_2$ or freeze-drying was performed. These dry materials were first analyzed in terms of density, porosity, specific surface area and morphology. Then, uniaxial compression tests were performed and analyzed in correlation with materials' dimensions, morphology and density.

2. Experimental

2.1. Materials

Microcrystalline cellulose (Avicel®, pH-101, degree of polymerization (DP) 180 as given by the manufacturer) was purchased from Sigma Aldrich. Cotton linters of two different DP,

810 and 1720, were kindly provided by Prof. Bodo Saake (University of Hamburg, Germany); their DP was obtained using size exclusion chromatography and the concentration of hemicellulose was below 1%. Cellulose was dried at 50 °C under vacuum for at least two hours before the dissolution. [Emim][OAc] was purchased from BASF, and DMSO as well as absolute ethanol were from Fisher Chemical. Water was distilled.

2.2. Methods

Preparation of cellulose aerogels and cryogels

The preparation of cellulose aerogels and cryogels has already been described in detail for the case of microcrystalline cellulose (DP 180).[24] The same approach was applied for the preparation of aero- and cryogels based on cotton linters (DP 810 and 1720). Briefly, dried cellulose was dissolved in a mixture of DMSO/[Emim][OAc] (60/40 wt/wt) at concentrations ranging from 0.7 to 11 wt%, depending on cellulose DP. The solutions were then poured into cylindrical vials that served as molds, and covered with ethanol in order to form the cellulose network by coagulation and to remove the solvent. This was the precursor for both aerogels and cryogels as it is the first non-solvent which stabilizes the network and sets the network's morphology and crystallinity. To obtain cellulose cryogels, ethanol was replaced by water. Then, these "aquagels" were frozen from the bottom of each sample by contact with liquid nitrogen. The frozen materials were then immediately freeze-dried in the Cryotec Cosmos 80 freeze-dryer (cold trap temperature -80 °C, pressure 40 mTorr) for 48 h. To prepare cellulose aerogels, supercritical CO_2 drying was carried out in Separex S.A.S. (France) at 110 bar and 45 °C.

Bulk density

Bulk density, ρ_{bulk}, was measured using GeoPyc 1360 Envelope Density Analyzer from Micromeritics with the DryFlo® powder as fluid medium. The applied force was of 25 N and each sample was measured in 5 cycles. The standard deviation of the measured values is ±0.002 g/cm^3.

Porosity

Porosity was determined using bulk density and skeletal density, $\rho_{skeletal}$, according to the following equation:

$$Porosity\ (\%) = 1 - \frac{bulk\ density}{skeletal\ density} \quad (1)$$

where the skeletal density is the density of amorphous cellulose. As it will be shown in the Results section, the samples obtained here consisted of mainly amorphous cellulose which density is known to be 1.38 g/cm^3.[25]

Scanning electron microscopy (SEM)

Morphological analysis of cellulose aerogels and cryogels was performed using Zeiss SupraTM 40 FEG scanning electron microscope with secondary electron detector. The acceleration voltage was 3 kV. Prior the observations all the samples were metallized with 7 nm of platinum.

Specific surface area

Specific surface area was determined by measuring N_2-adsorption isotherm at 77 K with ASAP 2020 analyzer (Micromeritics) and using Brunauer, Emmett and Teller (BET) approach.[26] All samples were measured after being degassed for 5 h at 70 °C.

X-rays diffraction

X-rays diffraction patterns were obtained on Philips X'Pert Pro diffractometer equipped with θ/θ PW 3050/60 goniometer and a $Cu_{K\alpha}$ source operated at 45 kV and 30 mA. The diffraction angle 2θ was measured from 5° to 60° with 0.08° step in 9 min.

Mechanical properties

The surfaces of all aerogels and cryogels were polished with P320 sandpaper (grain size of *approx.* 46 μm) to obtain regular cylinders with smooth walls and parallel and planar upper and lower planes. The samples' height and diameter were of similar size (around 1-2 cm) in order to minimize shear that may appear in such heterogeneous materials in case if height is higher than diameter. The dimensions of all the samples were measured before and after compression using a high precision caliper. The mechanical properties of such prepared samples were studied under the uniaxial unconfined compression on Zwick BZ 2.5/TN1S testing machine equipped with 1 kN load cell. The compression was conducted at room temperature and ambient pressure at the compression rate of 1 mm/min. Teflon sheets were used to avoid friction between the tool and the sample's surface. All measurements were performed in triplicate.

3. Results and discussion

3.1. Aerogels' and cryogels' density, specific surface area and morphology

The representative examples of aerogels and cryogels prepared from the lowest and the highest concentrations of cellulose of each DP are shown in Figure 1. The higher cellulose DP, the lower its minimal concentration in solution allowing making a self-standing dry porous material. The reason is the decrease of polymer overlap concentration with the increase of molecular weight. For example, it was possible to prepare aerogels and cryogels from only 0.7 wt% of cellulose of DP 1720, while the lowest concentration that yielded monolithic samples was 1 wt% for DP 810 and 3 wt% for DP 180. However, higher molecular weight of cellulose hindered the preparation of more concentrated precursor solutions because of a strong increase of viscosity and the impossibility to remove all air bubbles formed when placing solution in the mold. Consequently, the highest concentration for DP 810 used here was 5 wt% and only 3 wt% in the case of DP 1720.

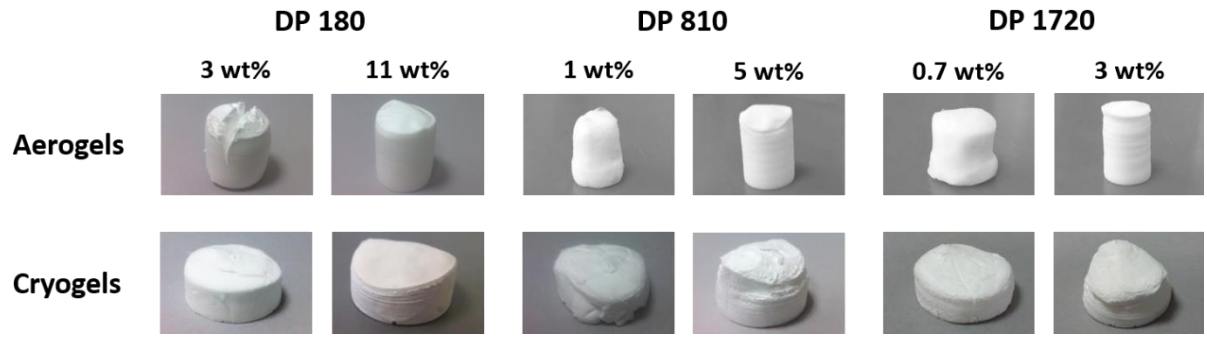

Figure 1: Non-polished aerogels and cryogels based on cellulose of different molecular weight from the lowest and the highest cellulose concentration of each DP.

Bulk densities ρ_{bulk} of all cellulose aerogels and cryogels are presented in Figure 2 as a function of cellulose concentration in solution. A theoretical density calculated for a hypothetical case of zero volume shrinkage is also shown for comparison. Bulk density increases with increasing cellulose concentration for all aerogels and cryogels from all DP, as expected and reported for various bio-aerogels.[3] Because of shrinkage during processing steps, the densities of all samples are higher than the corresponding theoretical density. Bulk density is also higher for aerogels than for cryogels. The increase of cellulose molecular weight leads to a higher density, both of cryo- and aerogels for the same concentration of cellulose in solution. However, because higher DP allows making self-standing cryo- and aerogels from lower cellulose concentration in solution, the density of cryogels can be very low, down to 0.016 g/cm^3 for DP 1720.

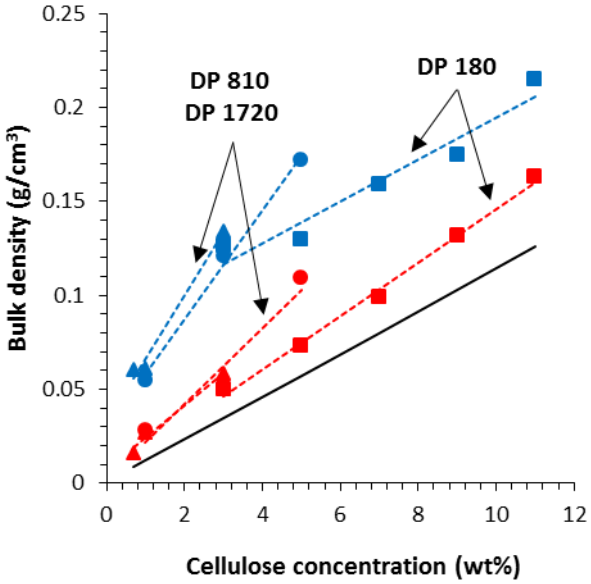

Figure 2: Bulk densities of aerogels (blue) and cryogels (red) from cellulose of different molecular weight as a function of cellulose concentration. Squares: DP 180; circles: DP 810; triangles: DP 1720. Solid line corresponds to the density in case of zero shrinkage; all dashed lines are linear trends.

Using the values of bulk density, porosity of each sample was calculated with the equation 1 (see Experimental section). The results are presented in Figure 3. As expected from density values, the porosity of cryogels is higher than that of aerogels, but all fall above 84%.

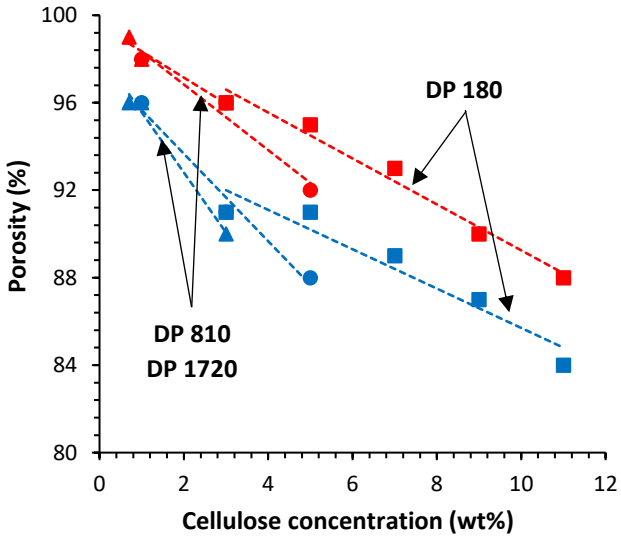

Figure 3: Porosity of aerogels (in blue) and cryogels (in red) from cellulose of different molecular weight as a function of cellulose concentration. Squares: DP 180; circles: DP 810; triangles: DP 1720. Dashed lines are linear trends.

The inner morphology of cellulose aerogels and cryogels observed by SEM is shown in Figure 4. The aerogels and cryogels shown in this figure are based on cellulose of different DP of the same concentration in solution of 3 wt%. As already reported,[24] the inner morphology of porous cellulose materials strongly depends on the drying technique. Drying with $scCO_2$ results in a cauliflower-like structure when cellulose is dissolved in [Emim][OAc] (with or without co-solvents): it is a network of small shaggy beads assembled together that have a finely nanostructured fibrous texture. This is the sign of a phase separation occurring via a spinodal decomposition when the cellulose solution is directly coagulated in a non-solvent, as suggested by Sescousse *et al.* and Demilecamps *et al*.[13,27] SEM images show that the size of the beads decreases with the increase of cellulose DP, similarly to their decrease with the increase of cellulose concentration.[24] Unfortunately, as already mentioned in the Introduction section, it is not possible to obtain a complete pore's size distribution in cellulose aerogels, and in bio-aerogels in general.

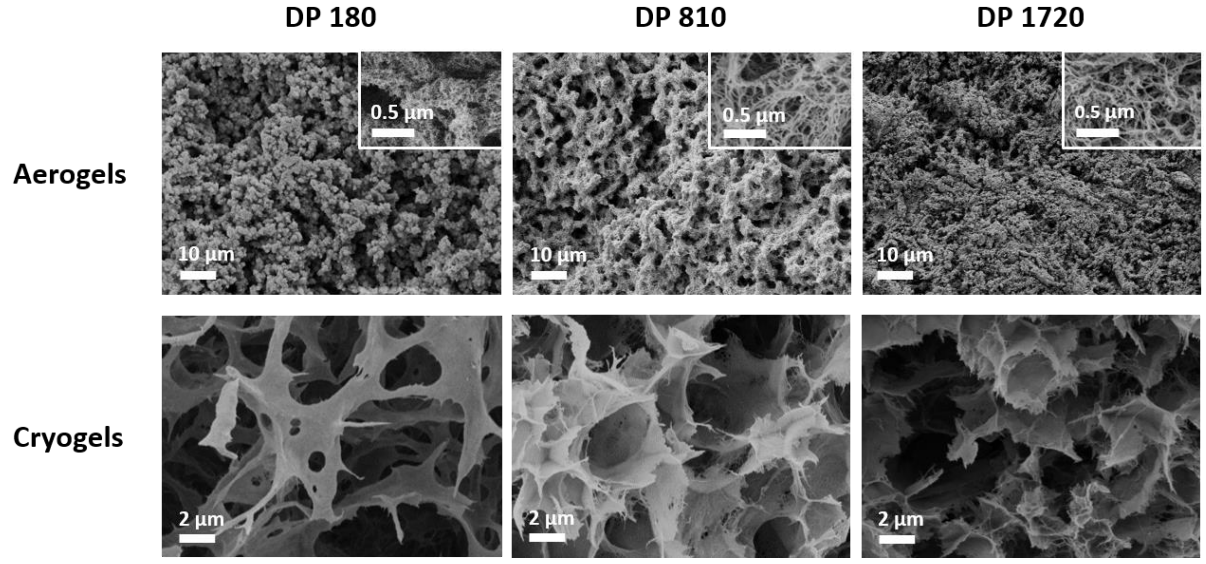

Figure 4: SEM images of aerogels and cryogels based on 3 wt% of cellulose of various DP.

Freeze-drying leads to a cellulose network with large and interconnected pores and pore walls being partly sheet-like.[24,28] The morphology is somehow similar to that of freeze-dried nanofibrillated cellulose if no precautions are taken to avoid the growth of ice crystals.[29,30] The reason of this similarity is that the pores replicate the shape of ice crystals which are destroying the nanostructure of pore walls by “squeezing” cellulose nanofibrils in pore walls. The pores are of several microns in diameter as can be deduced from Figure 4 and reported in our previous work for cryogels based on dissolved microcrystalline cellulose (DP 180).[24] With the increase of cellulose DP, more fibrous areas appear in the pore walls; we hypothesize that cellulose of higher DP can better withstand the growth of ice crystals during the freezing step.

The qualitative observations of aerogels’ and cryogels’ morphology were confirmed by the BET specific surface area measurements. The results are presented in Figure 5. All aerogels possess much higher specific surface area than cryogels. The specific surface area of aerogels made from cellulose of higher DP is slightly lower than that of aerogels based on cellulose of DP 180. In contrast, higher cellulose DP leads to much higher BET specific surface areas in cryogels. Drying with supercritical CO_2 allows the best preservation of network morphology while freeze-drying from water is severely distorting pores’ geometry by the growth of ice crystals. As cellulose of higher DP seems to better resist these stresses, the pores in the corresponding cryogels are smaller and the walls are more fibrous, as confirmed by SEM images in Figure 4.

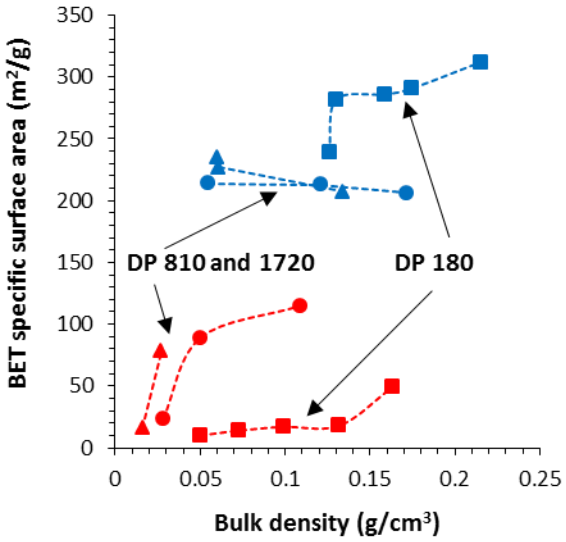

Figure 5: BET specific surface area of aerogels (in blue) and cryogels (in red) from cellulose of different molecular weight as a function of material's bulk density. Squares: DP 180; circles: DP 810; triangles: DP 1720. Dashed lines are given to guide the eye.

Except the case of aerogels based on cellulose of higher DP (DP 810 and 1720), the specific surface area increases with the increase of material's density or cellulose concentration in solution (see also Figure S1 in the Supplementary Information), both for aerogels and cryogels. This phenomenon is especially pronounced for cryogels based on cellulose of DP 810 and 1720 in which specific surface area increases from few tens to more than one hundred m^2/g with cellulose concentration in solution varying from 1 to 5 wt% (see Figure S1). It was suggested that the increase of cellulose concentration leads to a ''division'' of pores into smaller ones keeping the pore wall thickness more or less unchanged.[24]

Examples of X-rays diffraction patterns corresponding to the aerogel and cryogel based on cellulose of DP 180 are demonstrated in Figure S2 in the Supplementary Information and compared to that of neat microcrystalline cellulose (DP 180). Both cryogel and aerogel show a very broad peak centered at around 20.8° (Figure S2). The latter indicates that our aerogels and cryogels contain mostly amorphous cellulose. This result is in line with previously reported transformation of native crystalline cellulose I into amorphous cellulose

after its dissolution and subsequent coagulation in a non-aqueous non-solvent. This was the case for cellulose dissolved in ionic liquids 1-butyl-3-methylimidazolium chloride[31,32] and [Emim][OAc],[33] in SO_2-diethylamine-dimethylsulfoxide[34] and in DMSO-paraformaldehyde.[35]

3.2 Mechanical properties

The mechanical properties of cellulose aerogels and cryogels were tested under the uniaxial unconfined compression mode. Typical nominal stress-strain curves obtained for aerogels and cryogels from dissolved cellulose of DP 180 are shown in Figure 6. Similar results were obtained for all the other investigated cellulose aero- and cryogels.

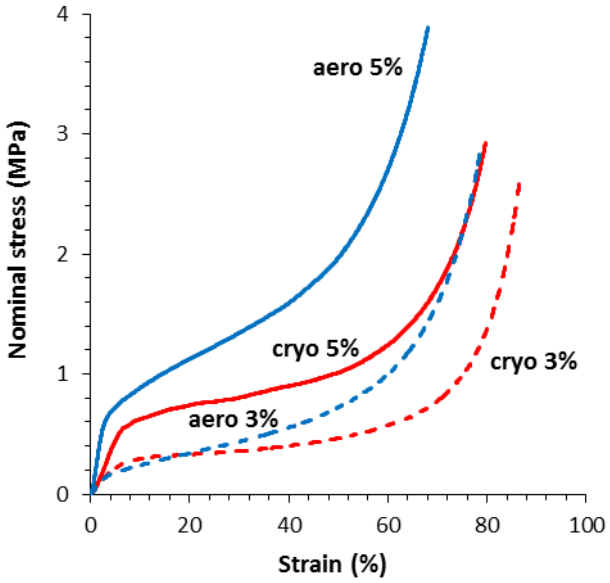

Figure 6: Typical stress-strain curves obtained for cryogels (red) and aerogels (blue) from 3 and 5 wt% dissolved cellulose of DP 180.

As already reported for various bio-aerogels[3,9,13], stress-strain curves consist of a linear elastic region at low strains allowing determination of compressive modulus *E*, a stress plateau corresponding to a progressive buckling of cell walls, and a densification of the material at high strains where the stress increases abruptly. Figure 6 may give the impression that for the same cellulose concentration in solution, aerogels are “stronger” than

cryogels. However, we need to recall here that their densities are different (Figure 2). The influence of the density on the material's mechanical properties will be discussed further.

The Poisson's ratio for bio-aerogels is very rarely reported. But, if considered, it is said to be zero.[9,13,21,22] We carefully examined the diameter of our aerogels and cryogels before and after the compression. The diameter of cryogels remains unchanged, which means that their Poisson's ratio is indeed very close to zero. However, this turned out not to be true for aerogels whose diameter expands under compression. Ideally, the Poisson's ratio should be determined in the elastic region. For example, for an incompressible elastic material at low strains it is equal to 0.5. Here, we determined the Poisson's ratio at high strains with the goal to demonstrate that it is not always zero. In the Figure 7, the Poisson's ratio is plotted *vs.* aerogel's compressive modulus with an inset showing aerogel's relative diameter ΔD as a function of aerogel's density for all aerogel samples prepared in this work:

$$\Delta D = \frac{D_{final} - D_0}{D_0} \quad (2)$$

where D_{final} and D_0 are the sample's diameter after and before compression, respectively.

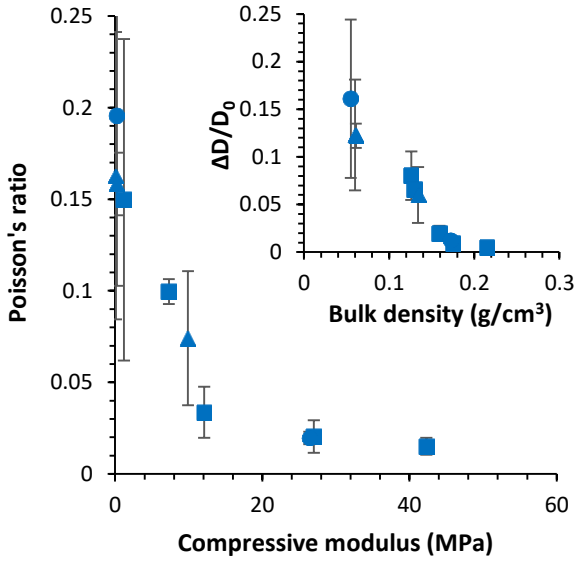

Figure 7: Poisson's ratio of aerogels from cellulose of different molecular weight as a

function of the corresponding compressive modulus; inset: relative diameter (eq. 2) as a function of aerogel's density. Squares: DP 180; circles: DP 810; triangles: DP 1720.

The inset in Figure 7 shows that the relative diameter is not zero especially for aerogels of low densities (or high porosities) and it decreases with the increase of density (decrease of porosity) for all the aerogels studied here. As a consequence, the Poisson's ratio is not zero for aerogels with low compressive modulus, the latter being power-law dependent on density as it will be discussed below. Moreover, we observed a decrease of the Poisson's ratio with the increase of modulus, all data roughly falling on a master plot. At higher modulus, the Poisson's ratio is close to zero as reported previously.[9,13,21,22]

Ashby and Gibson demonstrated that the Poisson's ratio of closed and open-cell polyurethane foams does not depend on material's density.[36] On the contrary, a decrease of Poisson's ratio with density increase was predicted for open-cell foams[37] and this trend was confirmed for polyurethane and carbon foams to occur mainly at low densities.[38] Modeling by using finite element analysis showed that the Poisson's ratio may decrease with increasing foam density,[39,40] the extent of the decrease depending on the degree of the foam regularity.[40]

For classical silica aerogels, the Poisson's ratio is around 0.205 to 0.22 and does not vary with density as demonstrated by measuring the longitudinal and transverse sound velocity.[41] The value of 0.2 was then used in the majority of subsequent publications for the theoretical and experimental studies of aerogels.[16,18,42] For other silica-based aerogels, the Poisson's ratio was reported to be slightly lower: 0.13-0.14 for methyltriethoxysilane-based aerogels,[43] 0.17 for tetramethoxysilane-based aerogels[6] and 0.16 for isocyanate-crosslinked silica aerogels.[44] For graphene aerogels, the Poisson's ratio varied from positive (0 to 0.4) to negative values (0 to -0.3).[45]

The dependence of the Poisson's ratio on the aerogel's modulus (and density) is important to consider if willing to model and predict bio-aerogel's mechanical properties. Still much more detailed experimental investigations of their mechanical properties and better

understanding of their morphology are needed: for example, shear and elastic moduli should be determined as it was done for silica aerogels, and the connectivity and fraction of dangling ends estimated. Sample's geometry must be carefully selected for each test in order to avoid artefacts and misinterpretations. Cellulose crystallinity, if any, should also be taken into account.

The compressive modulus and yield stress (taken at the end of the elastic regime) are presented in Figure 8 as a function of aerogel's and cryogel's bulk density. All cryogels show higher modulus and yield stress than aerogels at the same density. This can be explained by different material's morphology, recall Figure 4. While aerogels are made of "hairy beads" assembled together, pore walls of cryogels are partly sheet-like and may better resist the compression stresses.

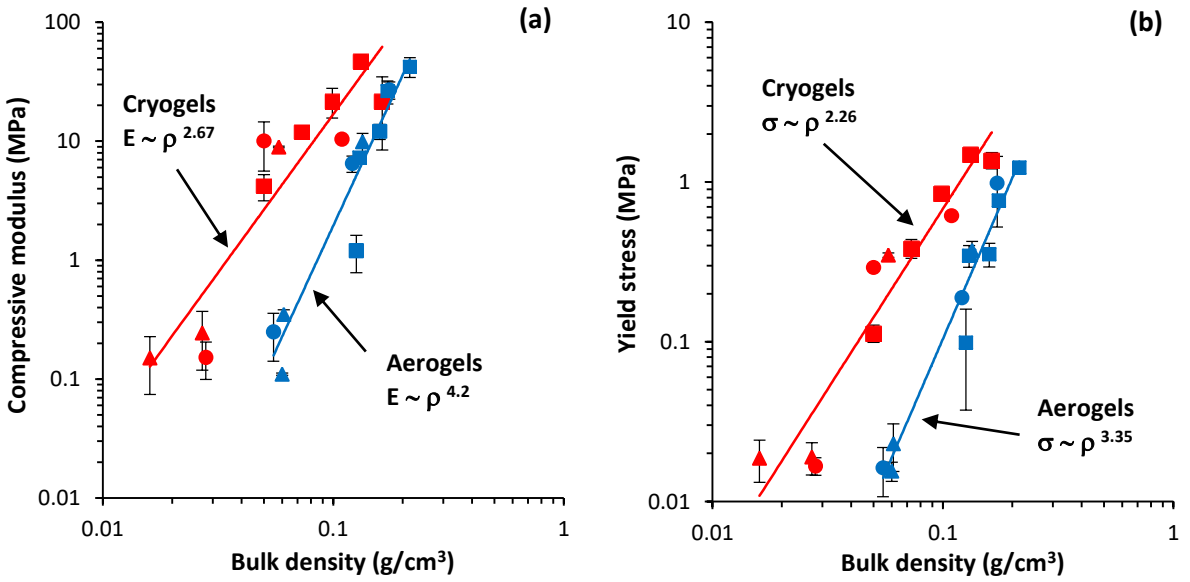

Figure 8: Compressive modulus (a) and yield stress (b) of aerogels (blue) and cryogels (red) from cellulose of different molecular weight as a function of material's density. Squares: DP 180; circles: DP 810; triangles: DP 1720. Lines are power law trends.

The compressive modulus and yield stress increase with bulk density ρ_{bulk}, following a power law dependence ~ ρ^n as predicted for foams[17] and also observed for aerogels, both

organic and inorganic.[6,15,16,18-20] This behavior is applicable to both types of porous cellulose materials studied here. As displayed in Figure 8, two master plots can be obtained for aerogels and for cryogels. In the case of aerogels, the exponent *n* for the compressive modulus *vs.* density is around 4 (Figure 8a); *n* = 3 – 4 was already reported for other cellulose aerogels obtained via dissolution-coagulation route.[13,14] For various synthetic polymer and silica aerogels, *n* was reported to vary from 2 to 4.[16,20,46,47] For silica aerogels, it was shown that the exponent strongly depends on the network connectivity which may change under compression.[6,7] For cryogels, the exponent *n* for the compressive modulus *vs.* density is around 2.7. According to Figure 4, cryogels can be very roughly seen rather as non-ideal open-cell foams in terms of their morphology. The exponent around 2 was also reported for other polysaccharide-based cryogels (1.6 for chitosan and 1.9 for xanthan).[48] The influence of cellulose molecular weight on aero- and cryogel's mechanical properties seems to be less pronounced than the influence of their density and morphology. Higher exponent in yield stress *vs.* density was also observed for aerogels as compared to cryogels (Figure 8b).

A comparison of compressive modulus *vs.* bulk density of aerogels made from dissolved-coagulated cellulose reported in literature and those obtained in this work is provided in Figure 9 (there is no data in literature on analogous cellulose cryogels' mechanical properties). Data scatter a lot with modulus varying in two orders of magnitude for the same material density. Cellulose aerogels are far from being ideal networks and their properties (morphology, density, crystallinity) depend on numerous preparation parameters. For example, they can be a network of "nanofibers" [21,22,49,50] or a network of hairy beads as observed here and by other authors.[13,51] Probably because of this large variety of morphologies and, most probably, crystallinities (that are very rarely analyzed), very different exponents in the power law of compressive modulus *vs.* density were reported (see a comparative Table S1 in Supplementary Information): from 1.5 to 4.7 [9,13,14,22,52,53] except one case where a linear dependence was claimed.[21]

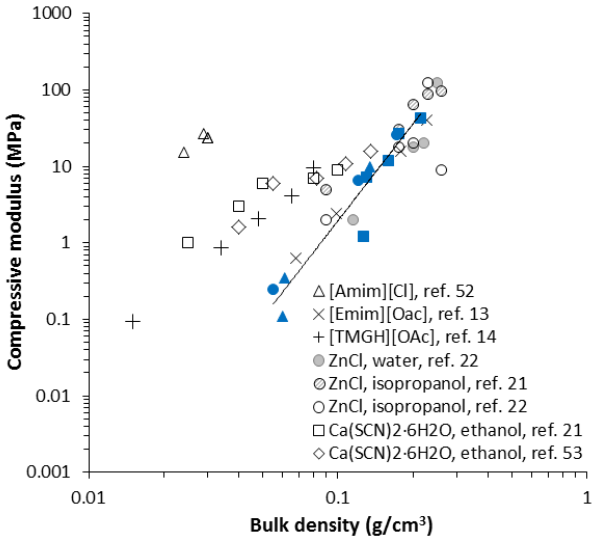

Figure 9: Summary of compressive modulus *vs.* aerogel's bulk density: results from literature (only data providing at least three values of modulus *vs.* density for the same formulation are considered) and from the current work (in blue). Symbols for the current results are the same as in Figure 8. Line is the linear trend found in this work.

Therefore, there is still a lot of work to do in the understanding of cellulose aerogels' mechanical properties, starting with carefully controlled experiments to full characterization of the materials obtained, including their crystallinity. Modeling of mechanical properties of cellulose aerogels is thus very challenging. Various mechanical solicitations (pure shear, isostatic compression, loading-unloading and measurements of strain recovery, etc.) followed by monitoring of the evolution of porous morphology and stress distribution in the samples would be very helpful for a better understanding of the mechanical properties of these porous cellulose materials.

4. Conclusions

Cellulose of various molecular weights and concentrations was dissolved in a mixture of ionic liquid and DMSO, coagulated in ethanol and highly porous amorphous materials were prepared using two drying methods: with $scCO_2$ (aerogels) and freeze-drying (cryogels). The main goal of this work was to correlate the aerogels' and cryogels' mechanical properties

under the uniaxial compression with their morphology and density. It was demonstrated that the generally accepted zero Poisson's ratio of cellulose-based aerogels does not hold true for low-density aerogels. Compressive modulus and yield stress of aerogels and cryogels were analyzed as a function of material's density and using existing theoretical and semi-empirical approaches. Cellulose cryogels can be roughly seen as non-ideal open-cell foams with modulus depending on material's density in power 2.5 - 3. Cellulose aerogels follow the trends reported for inorganic and synthetic polymeric aerogels with exponent around 4. At the same density, cellulose cryogels possess higher compressive modulus and higher yield stress than cellulose aerogels made from the same precursors. The reason is the difference in material's morphology, sheet-like *vs.* hairy beads, respectively.

Acknowledgments

This work was performed in the frame of the European project ''AEROWOOD'', WoodWisdom Net+ EC program, and supported by French ministry of agriculture, food processing and fishing.

References

1 K. J. De France, T. Hoare and E. D. Cranston, *Chem. Mater.*, 2017, **29**, 4609-4631.

2 N. Lavoine and L. Bergström, *J. Mater. Chem. A*, 2017, **5**, 16105-16117.

3 T. Budtova, *Cellulose*, 2019, **26**, 81-121.

4 H. Sehaqui, Q. Zhou, O. Ikkala and L. A. Berglund, *Biomacromolecules*, 2011, **12**, 3638-3644.

5 C. Jiménez-Saelices, B. Seantier, B. Cathala and Y. Grohens, *Carbohydr. Polym.*, 2017, **157**, 105-113.

6 T. Woignier, J. Reynes, A. Hafidi Alaoui, I. Beurroies and J. Phalippou, *J. Non-Cryst. Solids*, 1998, **241**, 45-52.

7 H.-S. Ma, A. P. Roberts, J. H. Prevost, R. Jullien and G. W. Scherer, *J. Non-Cryst. Solids*, 2000, **277**, 127-141.

8 M. Robitzer, F. Di Renzo and F. Quignard, *Microporous Mesoporous Mater.*, 2011, **140**, 9-16.

9 C. Rudaz, R. Courson, L. Bonnet, S. Calas-Etienne, H. Sallée and T. Budtova, B*iomacromolecules*, 2014, **15**, 2188-2195.

10 S. Groult and T. Budtova, *Carbohydr. Polym.*, 2018, **196**, 73-81.

11 H. Sehaqui, M. Salajková, Q. Zhou and L. A. Berglund, *Soft Matter*, 2010, **6**, 1824-1832.

12 H. Sehaqui, Q. Zhou and L. A. Berglund, *Compos. Sci. Technol.*, 2011, **71**, 1593-1599.

13 R. Sescousse, R. Gavillon and T. Budtova, *Carbohydr. Polym.*, 2011, **83**, 1766-1774.

14 S. F. Plappert, J.-M. Nedelec, H. Rennhofer, H. C. Lichtenegger, S. Bernstorff and F. W. Liebner, *Biomacromolecules*, 2018, **19**, 4411-4422.

15 R. W. Pekala, C. T. Alviso and J. D. LeMay, *J. Non-Cryst. Solids*, 1990, **125**, 67-75.

16 G. W. Scherer, D. M. Smith, X. Qiu and J. M. Anderson, *J. Non-Cryst. Solids*, 1995, **186**, 316-320.

17 L. J. Gibson and M. F. Ashby, *Cellular solids. Structure and properties*, Cambridge University Press, Cambridge, 1997.

18 A. H. Alaoui, T. Woignier, G. W. Scherer and J. Phalippou, *J. Non-Cryst. Solids*, 2008, **354**, 4556-4561.

19 L. Weigold and G. Reichenauer, *J. Non-Cryst. Solids*, 2014, **406**, 73-78.

20 J. C. H. Wong, H. Kaymak, S. Brunner and M. M. Koebel, *Microporous Mesoporous Mater.*, 2014, **183**, 23-29.

21 A. Rege, M. Schestakow, I. Karadagli, L. Ratke and M. Itskov, *Soft Matter*, 2016, **12**, 7079-7088.

22 M. Schestakow, I. Karadagli and L. Ratke, *Carbohydr. Polym.*, 2016, **137**, 642-649.

23 K. Ganesan, A. Barowski, L. Ratke and B. Milow, *J. Sol-Gel Sci. Technol.*, 2019, **89**, 156-165.

24 N. Buchtová and T. Budtova, *Cellulose*, 2016, **23**, 2585-2595.

25 K. Mazeau and L. Heux, *J. Phys. Chem. B*, 2003, **107**, 2394-2403.

26 S. Brunauer, P. H. Emmett and E. Teller, *J. Am. Chem. Soc.*, 1938, **60**, 309-319.

27 A. Demilecamps, C. Beauger, C. Hildenbrand, A. Rigacci and T. Budtova, *Carbohydr. Polym.*, 2015, **122**, 293-300.

28 K. N. Onwukamike, L. Lapuyade, L. Maillé, S. Grelier, E. Grau, H. Cramail and M. A. R. Meier, *ACS Sustain. Chem. Eng.*, 2019, **7**, 3329-3338.

29 F. Martoïa, T. Cochereau, P. J. J. Dumont, L. Orgéas, M. Terrien and M. N. Belgacem, *Mater. Des.*, 2016, **104**, 376-391.

30 A. Mulyadi, Z. Zhang and Y. Deng, *ACS Appl. Mater. Interfaces*, 2016, **8**, 2732-2740.

31 X. Cao, X. Peng, S. Sun, L. Zhong, S. Wang, F. Lu and R. Sun, *Carbohydr. Polym.*, 2014, **111**, 400-403.

32 Z. Ling, S. Chen, X. Zhang, K. Takabe and F. Xu, *Sci. Rep.*, 2017, **7**, 10230.

33 Å. Östlund, A. Idström, C. Olsson, P. T. Larsson and L. Nordstierna, *Cellulose*, 2013, **20**, 1657-1667.

34 D. Ciolacu, F. Ciolacu and V. I. Popa, *Cellulose Chem. Technol.*, 2011, **45**, 13-21.

35 L. R. Schroeder, V. M. Gentile and R. H. Atalla, *J. Wood Chem. Technol.*, 1986, **6**, 1-14.

36 L. J. Gibson and M. F. Ashby, *Proc. R. Soc. A*, 1982, **382**, 43-59.

37 W. E. Warren and A. M. Kraynik, *J. Appl. Mech.*, 1988, **55**, 341-346.

38 S. Sihn and A. K. Roy, *J. Mech. Phys. Solids*, 2004, **52**, 167-191.

39 H. X. Zhu, J. F. Knott and N. J. Mills, *J. Mech. Phys. Solids*, 1997, **45**, 319-343.

40 H. X. Zhu, J. R. Hobdell and A. H. Windle, *Acta Mater.*, 2000, **48**, 4893-4900.

41 J. Gross, G. Reichenauer and J. Fricke, *J. Phys. D: Appl. Phys.*, 1988, **21**, 1447-1451.

42 R. Pirard and J.-P. Pirard, *J. Non-Cryst. Solids*, 1997, **212**, 262-267.

43 D. Y. Nadargi, S. S. Latthe, H. Hirashima and A. V. Rao, *Microporous Mesoporous Mater.*, 2009, **117**, 617-626.

44 H. Luo, H. Lu and N. Leventis, *Mech. Time-Depend. Mater.*, 2006, **10**, 83-111.

45 X. Xu, Q. Zhang, Y. Yu, W. Chen, H. Hu and H. Li, *Adv. Mater.*, 2016, **28**, 9223-9230.

46 T. Woignier, J. Phalippou and R. Vacher, *J. Mater. Res.*, 1989, **4**, 688-692.

47 N. Diascorn, S. Calas, H. Sallée, P. Achard and A. Rigacci, *J. Supercrit. Fluids*, 2015, **106**, 76-84.

48 P. V. O. Toledo and D. F. S. Petri, *Int. J. Biol. Macromol.*, 2019, **123**, 1180-1188.

49 J. Cai, S. Kimura, M. Wada, S. Kuga and L. Zhang, *ChemSusChem*, 2008, **1**, 149-154.

50 R. Gavillon and T. Budtova, *Biomacromolecules*, 2008, **9**, 269-277.

51 N. Pircher, L. Carbajal, C. Schimper, M. Bacher, H. Rennhofer, J.-M. Nedelec, H. C. Lichtenegger, T. Resenau and F. Liebner, *Cellulose*, 2016, **23**, 1949-1966.

52 Q.-Y. Mi, S.-R. Ma, J. Yu, J.-S. He and J. Zhang, *ACS Sustain. Chem. Eng.*, 2016, **4**, 656-660.

53 l. Karadagli, B. Schulz, M. Schestakow, B. Milow, T. Gries and L. Ratke, *J. Supercrit. Fluids*, 2015, **106**, 105–114.

Supplementary Information

Mechanical properties of cellulose aerogels and cryogels

Nela Buchtová[1], Christophe Pradille[2], Jean-Luc Bouvard[1], Tatiana Budtova[1]*

1 - MINES ParisTech, CEMEF - Centre de Mise en Forme des Matériaux, CNRS UMR 7635, PSL Research University, CS 10207 rue Claude Daunesse, 06904 Sophia Antipolis, France

2 - Mat Xper, 19 Traverse du Barri, 06560, Sophia Antipolis, France

Corresponding author: Tatiana Budtova

E-mail: tatiana.budtova@mines-paristech.fr

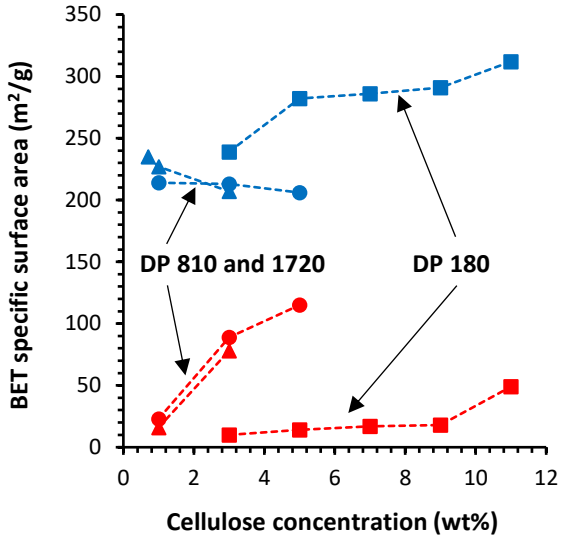

Figure S1: BET specific surface area of aerogels (in blue) and cryogels (in red) from cellulose of different molecular weight as a function of cellulose concentration. Dashed lines are given to guide the eye.

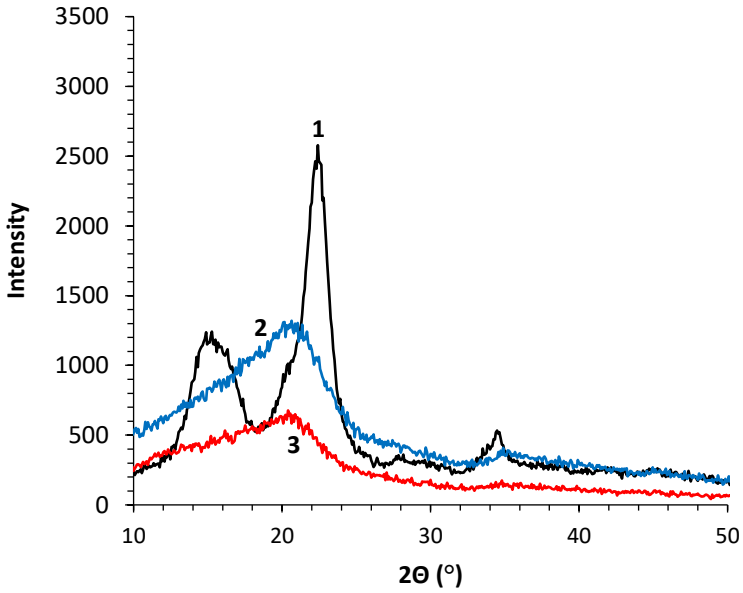

Figure S2: X-rays diffraction patterns of neat microcrystalline cellulose of DP 180 (1), aerogel based on 9 wt% of cellulose DP 180 (2) and cryogel based on 3 wt% of cellulose DP 180 (3).

Table S1: Summary of the results on the mechanical properties of cellulose aerogels obtained via dissolution-coagulation route (data from literature and the present work). Literature data were analyzed by plotting and approximating compressive modulus (E) *vs.* bulk density (ρ) with power law dependence.

Cellulose DP	Solvent	Non-solvent	Bulk density interval (g/cm^3)	Exponent n in $E \sim \rho^n$ dependence	Comment	Reference
Cotton, DP not reported	1-allyl-3-methylimidazolium chloride ([Amim][Cl])	Water and water/[Amim][Cl] mixture	0.024 – 0.03	2.15		52
DP 211	$Ca(SCN)_2 \cdot 6H_2O$	Ethanol	0.04 – 0.014	1.67		53
DP 211	$Ca(SCN)_2 \cdot 6H_2O$	Ethanol	0.03 – 0.1	1.51	Authors report linear dependence	21
DP 211	ZnCl	Isopropanol	0.09 – 0.26	2.94	Authors report aerogels composed of cellulose I and linear dependence of modulus *vs.* density	21
DP 211	ZnCl	Isopropanol	0.09 – 0.26	2.55		22
DP 211	ZnCl	Water	0.08 – 0.25	4.69		22
DP 180	[Emim][OAc]	Water	0.06 – 0.22	3.38		13
Eucalyptus prehydrolysis kraft dissolving pulp, DP 1013	1,1,3,3-tetramethylguanidinium acetate [TMGH][OAc]	Ethanol	0.015 – 0.08	2.69	Crystallinity 72%, axially anisotropic	14
DP 180, 810 and 1720	[Emim][OAc]/DMSO	Ethanol	0.06 – 0.22	4.20	Amorphous	This work